

**Broad H $\alpha$  Wing Formation in the Planetary Nebula IC 4997**

Hee-Won Lee and Siek Hyung

*Korea Astronomy Observatory,  
61-1, Whaam-dong, Yusong-gu,  
Taejon, 305-348, Korea*

hwlee@hanul.issa.re.kr

**ABSTRACT**

The young and compact planetary nebula IC 4997 is known to exhibit very broad wings with a width exceeding  $5000 \text{ km s}^{-1}$  around H $\alpha$ . We propose that the broad wings are formed through Rayleigh-Raman scattering involving atomic hydrogen, by which Ly $\beta$  photons with a velocity width of a few  $10^2 \text{ km s}^{-1}$  are converted to optical photons and fill the H $\alpha$  broad wing region. The conversion efficiency reaches 0.6 near the line center where the scattering optical depth is much larger than 1 and rapidly decreases in the far wings. Assuming that close to the central star there exists an unresolved inner compact core of high density,  $n_H \sim 10^{9-10} \text{ cm}^{-3}$ , we use the photoionization code ‘CLOUDY’ to show that sufficient Ly $\beta$  photons for scattering are produced. Using a top-hat incident profile for the Ly $\beta$  flux and a scattering region with a H I column density  $N_{HI} = 2 \times 10^{20} \text{ cm}^{-2}$  and a substantial covering factor, we perform a profile fitting analysis to obtain a satisfactory fit to the observed flux. We briefly discuss the astrophysical implications of the Rayleigh-Raman processes in planetary nebulae and other emission objects.

*Subject headings:* planetary nebulae — planetary nebulae : individual IC 4997 — radiative transfer — scattering — profile

**1. Introduction**

With the advent of the Hubble Space Telescope and large optical telescopes, planetary nebulae (PNe) came to be known to possess complex structures including multiple shells and collimated outflows, of which the origins still remain puzzling (e.g. Gurzadyan 1997). In addition, PNe display various nebular morphology ranging from elliptical to spherical, bipolar (or of butterfly shape), point-symmetrical and irregular. However, the physical explanation for the morphological diversity is not found (e.g. Corradi & Schwarz 1995).

Noting that symbiotic stars, widely known to be binary systems of a cool giant and a hot white dwarf or a main sequence star, exhibit bipolar emission nebulae, Soker (1998) advocated the view that the bipolar morphology in planetary nebulae is attributed to the binarity in the central star system. Evolutionary links between symbiotic stars and PNe have been also proposed by a number of researchers (e.g. Corradi 1995). Currently one of the most controversial issues is the existence of an accretion disk in symbiotic stars and bipolar PNe. According to the recent SPH computations by Mastrodemos & Morris (1998), in a detached binary system consisting of a mass losing giant and a companion star, the slow and dusty stellar wind from the giant may induce the formation of an accretion disk around the companion star (see also Theuns et al. 1996).

Circumstantial evidence supporting this scenario was provided by Lee & Park (1999), who proposed that a disk type emission model can naturally explain the main characteristics of the profiles and the polarized fluxes of the Raman-scattered 6830 and 7088 Å features in the symbiotic star RR Tel. The Raman scattering process by atomic hydrogen has been introduced by Schmid (1989), who identified the 6830 and 7088 Å bands in symbiotic stars as the Raman scattered O VI 1032, 1038 doublet. A thick H I component around the giant companion in a symbiotic star is believed to act as the Raman-scatterer which converts the UV continuum around  $\text{Ly}\beta$  into the optical continuum.

The young and compact PN IC 4997 is particularly interesting in that it also displays a hint of bipolar morphology, as is revealed in the radio image presented by Miranda & Torrelles (1998). Miranda et al. (1996) presented spectroscopy of IC 4997 which shows very broad wings around  $\text{H}\alpha$  with FWHM  $5375 \text{ km s}^{-1}$ . IC 4997 is not the only PN showing the broad  $\text{H}\alpha$  wings. The bipolar planetary nebula M 2-9 is also known to exhibit extremely broad wings with width  $\sim 10^4 \text{ km s}^{-1}$  in  $\text{H}\alpha$  (Balick 1989, see also Torres-Peimbert & Arrieta 1998).

Patriarchi and Perinotto (1991) used the IUE data of 159 planetary nebulae to find that about 60 per cent of central stars have a stellar wind with a measured edge velocity ranging 600 to  $3500 \text{ km s}^{-1}$ . Feibelman (1982) presented IUE spectroscopy of IC 4997 and found no evidence of P-Cygni profile in C IV 1550 doublet, which strongly implies the absence of strong stellar winds around the central star. This makes it difficult to attribute the broad wing around  $\text{H}\alpha$  in IC 4997 to the kinematics associated with the fast stellar wind.

Electron scattering has been often invoked to explain the wing formation in luminous blue variables (Bernat & Lambert 1978). However, it does not appear to be the case in IC 4997 since the Thomson scattering cross section is independent of wavelength and therefore broad wings should be present around other emission lines. Furthermore, in a planetary nebula, it is difficult to incorporate an electron scattering component with the electron temperature  $T_e > 10^6 \text{ K}$  and a sufficient scattering optical depth.

An interesting observation of IC 4997 is provided by Altschuler et al. (1986), who reported the detection of H I in IC 4997 by observing the 21 cm absorption dip (see also Schneider et al. 1987). With a large amount of atomic hydrogen, the broad wings around  $\text{H}\alpha$  can be formed by

Rayleigh-Raman scattering, where the incident radiation in the vicinity of Ly $\beta$  converted to the radiation around H $\alpha$  with a width broadened by a factor of  $\lambda_{H\alpha}/\lambda_{Ly\beta} = 6.4$  due to the incoherency of the scattering process. In this Letter, we investigate the broad H $\alpha$  wing formation through the Rayleigh-Raman scattering process and discuss the implications on the astrophysics of bipolar planetary nebulae.

## 2. Model

### 2.1. Wing Formation from the Rayleigh-Raman Process

In this work, we adopt a simple model to investigate the wing formation through the Rayleigh-Raman process. We assume that the scattering region is in the form of a finite slab with the column density  $N_{HI}$  with the solid angle  $\Omega_s$  with respect to the radiation source, which coincides with the central star of the planetary nebula. We discuss the Ly $\beta$  line radiation source in the next subsection and now we assume that the scattering region is illuminated by a far UV radiation source with intensity  $I_\lambda$ .

A UV photon around Ly $\beta$  is incident on a hydrogen atom in the ground state  $1s$ , which subsequently de-excites either to the  $2s$  state re-emitting an optical photon around H $\alpha$  (Raman scattering) or to the  $1s$  state resulting in an outgoing UV photon with the same frequency (Rayleigh scattering). Depending on the scattering optical depth, a UV photon may suffer a number of Rayleigh scatterings followed by a Raman scattering and escape the scattering region, because the  $2s$  state is usually populated negligibly compared with the ground state.

The incident wavelength  $\lambda_i$  and the wavelength  $\lambda_o$  of the Raman-scattered radiation are related by the energy conservation,  $\lambda_i^{-1} = \lambda_o^{-1} + \lambda_{Ly\alpha}^{-1}$ , which yields the conversion of the wavelength interval

$$\Delta\lambda_o/\lambda_o = (\lambda_o/\lambda_i)(\Delta\lambda_i/\lambda_i). \quad (1)$$

Because of the factor  $\lambda_o/\lambda_i$ , UV photons with a width  $\Delta V_i$  centered at Ly $\beta$  are spread around H $\alpha$  with a broadened width  $\Delta V_o = 6.4\Delta V_i$ .

The number of UV photons incident on the scattering region per unit time per unit wavelength interval is given by  $I_{\lambda_i}(T_*)\pi R_*^2\Omega_s/(hc/\lambda_i)$ . We introduce the parameter  $C_R(\lambda_i)$ , which is the conversion factor from UV to optical through the Rayleigh-Raman scattering process. The conversion factor  $C_R(\lambda_i)$  depends sensitively on the wavelength and the column density as well as the detailed geometry of the scattering region, and can be computed using a Monte Carlo technique (see Lee & Yun 1998).

The number of Raman-scattered photons coming out from the region per unit time per unit wavelength interval is given by

$$N_{H\alpha} = [I_{\lambda_i}(T_*)\pi R_*^2\Omega_s/(hc/\lambda)]C_R(\lambda)\lambda_i^2/\lambda_o^2. \quad (2)$$

Therefore, the Raman-scattered flux is

$$\begin{aligned} F^{Ram}(\lambda) &= N_{H\alpha}(hc/\lambda)/r^2 \\ &= F^{UV}(\lambda_i) \times C_{eff} \end{aligned} \quad (3)$$

where  $F^{UV}(\lambda_i) \equiv [I_{\lambda_i} \pi R_*^2 / r^2]$  is the flux that would be observed from the radiation source with a size  $R_*$  located at a distance  $r$  and  $C_{eff} \equiv [\Omega_s C_R(\lambda_i) \lambda_i^3 / \lambda^3]$  is the effective Raman conversion efficiency.

## 2.2. Conversion Efficiency

In Fig. 1, we present the Raman conversion efficiency  $C_R(\lambda)$  for H I column densities  $N_{HI} = 10^{19}, 10^{20}$ , and  $10^{21} \text{ cm}^{-2}$ , using the Monte Carlo code developed by Lee & Yun (1998). In the optically thin regime, the single scattering approximation holds so that

$$C_R(\lambda) = \tau_{tot}(\sigma_{Ram}/\sigma_{tot}). \quad (4)$$

In the optically thick limit, the conversion rate is investigated by Lee & Lee (1997), who proposed an empirical relation

$$C_R(\lambda) = \sum_n r_\sigma f(n) / \sum_n [(1 - r_\sigma)\beta(n) + r_\sigma] f(n), \quad (5)$$

where  $r_\sigma \equiv \sigma_{Ram}/\sigma_{tot}$ . Here,  $\beta(n) \simeq \frac{1}{2}e^{-\sqrt{n}}$  is the escape probability from the  $n$ th scattering site, and  $f(n)$  is the photon number flux scattered no less than  $n$  times which is obtained recursively by

$$f(n+1) = (1 - r_\sigma)[1 - \beta(n)]f(n). \quad (6)$$

A direct substitution with  $r_\sigma = 0.11$  near the line center yields  $C_R(\lambda) = 0.6$ , which is in excellent agreement with the result shown in Fig. 1.

## 2.3. Photoionization Structures of the Emission Nebula

In this subsection we discuss the Ly $\beta$  flux that may enter the scattering region. Hyung et al. (1994) performed a photoionization computation to conclude that the observed emission lines are reproduced approximately using a model consisting of a thin shell of density  $n \sim 10^7 \text{ cm}^{-3}$  surrounded by a much larger shell with a much lower density  $\sim 10^4 \text{ cm}^{-3}$ . They also noted that the N III]  $\lambda 1754/\lambda 1749$  ratio may indicate the existence of a much denser region with  $n \geq 10^9 \text{ cm}^{-3}$  (e.g. see Czyzak et al. 1986).

We use the photoionization code ‘CLOUDY 90.05’ developed by Ferland (1996) to obtain the Ly $\beta$  flux that is expected around a central star of a PN. We fix the temperature and radius of the

central star to be  $T_* = 6 \times 10^4$  K,  $R_* = R_\odot$  and compute the hydrogen emission line fluxes for densities  $n = 10^6 - 10^{10}$  cm $^{-3}$ . According to Hyung et al. (1994) the observed H $\alpha$  luminosity is  $4 \times 10^{35}$  erg s $^{-1}$  assuming the distance  $d = 2.4$  kpc to IC 4997 and the interstellar extinction parameter  $C = \log I(\text{H}\beta)/F(\text{H}\beta) = 0.8$  where the observed flux  $F(\text{H}\beta)$  in H $\beta = 2.95 \times 10^{-11}$  ergs s $^{-1}$  cm $^{-2}$ .

In Table 1, we show the result. This shows that the observed H $\alpha$  flux is obtained from a region of density  $n \sim 10^7$  cm $^{-3}$ , for which we get a much smaller Ly $\beta$  flux. However, when  $n \sim 10^{9-10}$  cm $^{-3}$ , a much larger Ly $\beta$  flux is obtained. Therefore, if there exists an emission region of density  $n \sim 10^{9-10}$  cm $^{-3}$ , we may have a sufficient number of Ly $\beta$  photons to fill the H $\alpha$  wings. Furthermore, this region is plausibly located much closer to the central star than other emission regions are. Hence assuming that the distance is  $\sim 0.1$  AU, we may expect that there is a high velocity dispersion of order 100 km s $^{-1}$  in the region.

### 3. Result

In Fig. 2, by the dotted lines we show the H $\alpha$  wings expected from the Rayleigh-Raman processes. For the incident Ly $\beta$  flux we use  $L_{\text{Ly}\beta} = 6 \times 10^{35}$  erg s $^{-1}$ , which is expected to be obtained from an unresolved core of high density  $n \sim 10^{9-10}$  cm $^{-3}$  near the central star. We tested two types of profiles for the incident Ly $\beta$  flux, that is, a top-hat profile with a width of 300 km s $^{-1}$  and a Gaussian with the same velocity width. We present the results for the best-fitting column density of the scattering region which is  $N_{\text{HI}} = 2 \times 10^{20}$  cm $^{-2}$  for the incident top-hat profile and  $N_{\text{HI}} = 4 \times 10^{20}$  cm $^{-2}$  for the Gaussian profile. In this work, we concentrate only on the wing parts farther than 300 km s $^{-1}$  ( $\Delta\lambda > 6.5$  Å around H $\alpha$ ) from the line center.

Because the top-hat profile for the incident Ly $\beta$  provides an excellent fit to the observed H $\alpha$  wing profile, we expect that other types of input profiles can also produce a good fit except for some extreme cases. This is illustrated by another good fit using a Gaussian profile shown in Fig. 2(b). However, we realize the much higher column density, i.e. by a factor of 2, is required in the latter case.

In this work, the incident Ly $\beta$  flux was computed with a highly simplified assumption. An introduction of a velocity field in the emission region may alter drastically both the strength and the profile of the emergent line flux. Furthermore the scattering region is complex and consists of a number of components differing in column density and geometrical shape. Therefore, a better fit can be assured from composite scattering region models and more complicated radiative transfer, which are deferred to a future investigation. Since the extreme wings are formed by the scatterers located in the equatorial region, we predict stronger polarization in these regions than in the near center regions that are formed by scatterers distributed nearly spherically.

#### 4. Discussion

The exact location of the scattering region with  $N_{HI} = 10^{20} \text{ cm}^{-2}$  is not well-constrained from this analysis. If the bipolar morphology has originated from a binary central star system as in symbiotic stars advocated by Soker (1998), the binary companion of IC 4997 may provide a scattering site in the form of an extended stellar atmosphere or a slow and probably dusty stellar wind. This situation is often met in symbiotic stars, where a slow and thick wind from a giant companion may act as a Raman scattering site. In this picture, the column density of  $\sim 10^{20} \text{ cm}^{-2}$  is more plausibly attributed to the slow stellar wind.

In the bipolar planetary nebula M2-9, Balick (1989) observed the spectrum similar to that of the symbiotic star RR Tel. M2-9 might be the case of a binary central star system. Since there exists a thick circumstellar region in M2-9, the extremely wide  $H\alpha$  wings with a width  $11000 \text{ km s}^{-1}$  are likely to be formed through the Raman process in a scattering region of column density  $N_{HI} \sim 10^{21} \text{ cm}^{-2}$ .

Broad  $H\alpha$  wings are found in a number of post-AGB stars according to a recent report by Van de Steene et al. (1999), who excluded several theoretical possibilities as the wing formation mechanism including Thomson scattering and Rayleigh scattering. Considering that in post-AGB stars much H I can be found in the stellar wind region and/or in a dense torus surrounding the central star, it is very convincing that the broad  $H\alpha$  wings in these systems are also attributable to Rayleigh-Raman scattering. So far the Raman-scattering is unique to symbiotic stars and the only exception appears to be the young planetary nebula NGC 7027, from which a Raman-scattered He II line has been identified (Péquignot et al. 1997). From this study broad  $H\alpha$  wings are expected to be found in a hot and dense H II region surrounded by an H I region, where the conditions may be met in objects including symbiotic stars, supernova remnants, and galactic supershells.

Since the Rayleigh-Raman scattering provides a strong constraint on the amount of H I in the nebula, it can be an important tool in studying the mass loss process in the late stage of AGB evolution. Through high quality spectra around Balmer emission lines, the physical parameters of the central star can be estimated, which is complementary to the information obtained by other methods such as the Zanstra method. We also note that spectropolarimetry can provide more detailed structural information as mentioned in section 3.

HWL is grateful to Chul-Sung Choi and Hwankyung Sung for helpful comments and discussion. He also thanks the hospitality during his visit to the Korea Institute for Advanced Study. This research was supported in part by Star Research Grant through No. Star 99-2-500-00 to the KAO/BOAO sponsored by the Korea Ministry of Science and Technology.

## REFERENCES

- Altschuler, D. R., Schneider, S. E., Giovanardi, C., & Silverglate, P. R., 1986, *ApJ*, 305, L85
- Balick, B., 1989, *AJ*, 97, 476
- Bernat, A. P., and Lambert, D. L., 1978, *PASP*, 90, 520
- Corradi, R. L. M., 1995, *MNRAS*, 276, 521
- Corradi, R. L. M., & Schwarz, H. E., 1995, *A&A*, 293, 871
- Czyzak, S. J., Keyes, C. D., and Aller, L. H., 1986, *ApJ*, 61, 159
- Feibelman, W. A., 1982, *ApJ*, 258, 562
- Ferland, G., 1996, in Hazy, Univ. of Kentucky Dept. of Phys. and Astron. Internal Rep.
- Hyung, S., Aller, L. H., & Feibelman, W. A. 1994, *ApJS*, 93, 465
- Garzadyan, G. A., 1997, *The Physics and Dynamics of Planetary Nebulae* (Berlin: Springer-Verlag)
- Mastrodemos, N., & Morris, M., 1998, *ApJ*, 497, 303
- Lee, K. W., & Lee, H. -W., 1997, *MNRAS*, 292, 573
- Lee, H. -W., & Park, M. -G., 1999, *ApJ*, 515, L89
- Lee, H. -W., & Yun, J. -H., 1998, *MNRAS*, 301, 193
- Miranda, L. F., Torrelles, J. M., & Eiroa, C., 1996, *ApJ*, 461, L111
- Miranda, L. F., & Torrelles, J. M., 1998, *ApJ*, 496, 274
- Patriarchi, P., & Perinotto, M., 1991, *A&AS*, 91, 325
- Péquignot, D., Baluteau, J. -P., Morisset, C., & Boisson, C., 1997, *A&A*, 323, 217
- Schmid, H. M., 1989, *A&A*, 211, L31
- Schneider, S. E., Altschuler, D. R., & Giovanardi, C., 1987, *ApJ*, 314, 572
- Soker, N. 1998, *ApJ*, 496, 833
- Theuns, T., Boffin, H. M. J., & Jorissen, A., 1996, *MNRAS*, 280, 1264
- Torres-Peimbert, S., & Arrieta, A., 1998, *Revista Mexicana de Astronomia y Astrofisica Serie de Conferencias*, 7, 171

Van de Steene, G. C., Wood, P. R., and van Hoof, P. A. M., 1999, to appear in *Asymmetrical Planetary Nebulae II*, ASP Conference Series, eds. J. H. Kastner, N. Soker, & S. Rappaport, astro-ph/9910024



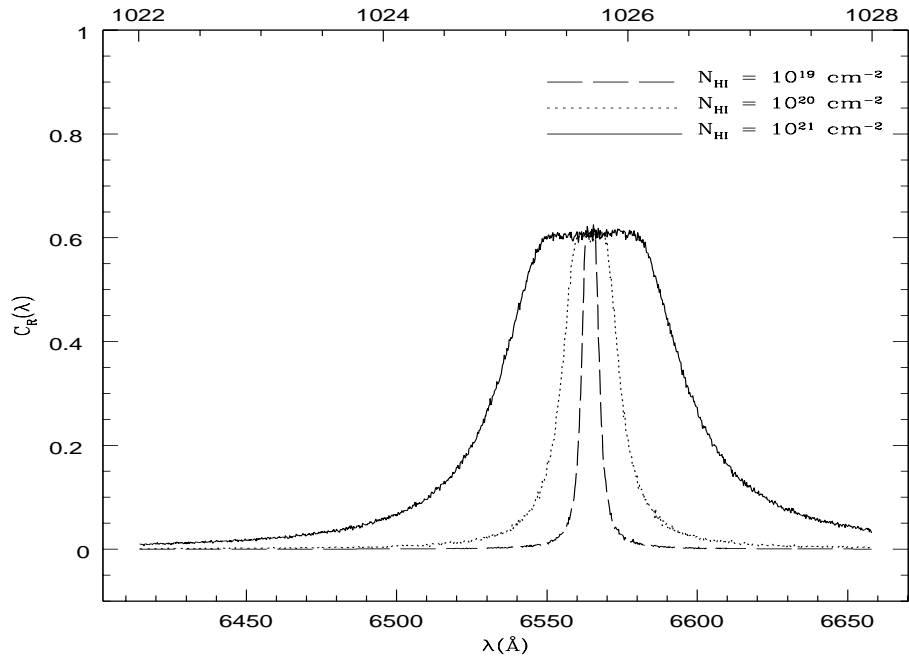


Fig. 1.— Raman conversion efficiency  $C_R(\lambda)$  for H I column densities  $N_{\text{HI}} = 10^{19}$  (solid line),  $10^{20}$  (dotted line), and  $10^{21} \text{ cm}^{-2}$  (long dashed line) obtained using a Monte Carlo technique. The horizontal (lower) axis is the outgoing wavelength around  $\text{H}\alpha$  and in the upper part is shown the incident wavelength around  $\text{Ly}\beta$ .

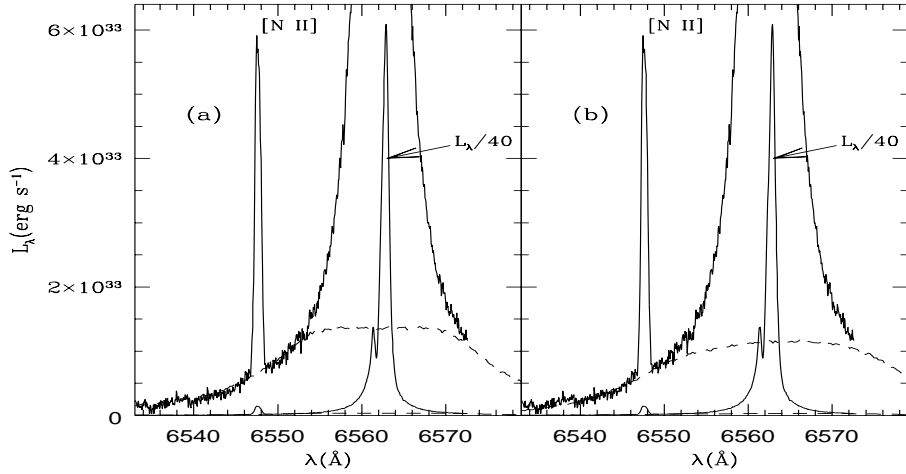


Fig. 2.— Observed flux around H $\alpha$  and the wings produced numerically in this work. The flux, represented by the solid line, was observed on August 31, 1991 UT, and is corrected for atmospheric and interstellar extinctions ( $C = 0.8$ ). The vertical axis represents the specific luminosity with the assumed distance 2.4 kpc to IC 4997. By the dotted lines we show the wings produced via Rayleigh-Raman scattering. We assumed that the total incident Ly $\beta$  flux  $L_{Ly\beta} = 6 \times 10^{35}$  erg s $^{-1}$ . In panel (a), the incident Ly $\beta$  has a top-hat profile with a width 300 km s $^{-1}$  and the H I column density of the scattering region  $N_{HI} = 2 \times 10^{20}$  cm $^{-2}$ . In panel (b), the incident profile is a Gaussian with the same width and the scattering region has  $N_{HI} = 4 \times 10^{20}$  cm $^{-2}$ . We also illustrate the flux multiplied by 1/40 to show the whole H $\alpha$  profile.

Table 1. H I emission line fluxes from a plasma photoionized by a PN central star with  $T_* = 6 \times 10^4$  K, and  $R_* = R_\odot$ .

$\log n^a$	$\log F_{Ly\alpha}$	$\log F_{Ly\beta}$	$\log F_{Ly\gamma}$	$\log F_{H\alpha}$	$\log F_{H\beta}$
10	36.849	35.687	35.154	35.382	34.988
9	36.944	35.233	34.544	35.874	35.451
8	36.957	34.025	33.135	35.957	34.991
7	36.961	33.268	33.043	35.890	35.318
6	36.953	33.146	33.049	35.875	35.380

<sup>a</sup>All quantities are measured in cgs units.

Note. — The photoionization code ‘CLOUDY 90.05’ (Ferland 1996) was used to obtain the result.